Synthesis and Properties of the Iron(II) Complex of a Pentadentate Ligand Derived from Diazaoxacyclononane

Witold S. Szulbinski, P. Richard Warburton, and Daryle H. Busch*

Department of Chemistry, University of Kansas, Lawrence, Kansas 66045

Nathaniel W. Alcock

Department of Chemistry, University of Warwick, Coventry CV4 7AL, United Kingdom

Received July 1, 1992

The pentadentate ligand DPC (DPC = 4,7-bis(2-picolyl)-4,7-diaza-1-oxacyclononane) reacts with $FeCl_2$ in MeOH to produce the high-spin ($S = 2$) iron(II) complex (λ_{max} = 260 and 378 nm in water). The structure of the complex was determined by X-ray crystallography. Crystal data: orthorhombic space group $P2_12_12_1$, a = 8.016 (3) Å, b = 13.188 (8) Å, c = 20.539 Å, U = 2171.3 Å^3, Z = 4, D_c = 1.69 cm^{-3}, Mo Kα radiation, λ = 0.710 69 Å, μ(Mo Kα) = 0.96 mm^{-1}, T = 290 K, and R = 0.049 for 1895 unique observed ($I/\sigma(I) \geq 2.0$) reflections. Cyclic voltammetry and chronoamperometry in MeCN revealed that the complex undergoes a reversible one electron redox process at $E_{1/2}$ = 0.71 V vs NHE ($D = 7.6 \times 10^{-6}$ cm^2/s). Moreover, ESR spectral studies identified the in situ electrochemically generated Fe(III) species as a high-spin complex, and electrochemical studies indicate 6-coordination for both the iron(II) and iron(III) species. In aqueous solution, for pH > 9, Fe(DPC)3$^+$ forms a hydroxo complex, as a result of which the iron(III/II) redox couple is shifted negative to 0.54 V vs NHE (pH = 9.6). Spectroelectrochemical measurements with a long optical path thin-layer cell containing parallel glassy-carbon working electrodes showed that, during the oxidation of Fe(DPC)$^{2+}$ in 2 M aqueous KCl, the MLCT absorption band at 378 nm disappears, with a concomitant increase in absorbance with λ_{max} = 310 nm, corresponding to the formation of [Fe(DPC)Cl]$^{2+}$.

Introduction

The unfolding of the macrocyclic coordination chemistry of the ligand triazacyclononane and its various analogs and derivatives has received much attention in recent years.[1] This unusual cyclic tridentate ligand must coordinate facially to the metal due to steric constraints, in contrast to other saturated polyazamacrocyclic ligands.[2] Of particular interest to our research group are complexes of iron and to a lesser extent cobalt and manganese, since many complexes of these elements may be viewed as simple models for the catalytic centers in a number of biological systems. In addition to iron(II) and iron(III) complexes of triazacyclononane, Fe([9]aneN3)$_2^{2+/3+}$,[3] other metal complexes have been synthesized with either ligating[4] or nonligating[5] pendant groups attached to the nitrogens or with one or more nitrogens replaced by another hetero atom, such as oxygen[6] or sulfur.[7] Much of the effort has been applied to determining the effects on the physical and chemical properties on the metal complexes that result from these changes in ligand structure.

In this paper the synthesis and characterization of (4,7-dipicolyl-4,7-diaza-1-oxacyclonane)iron(II) (Fe(DPC)$^{2+}$) are described. This complex contains a macrocyclic ring that is related to triazacyclononane by replacement of one of the nitrogens by an oxygen, and the remaining two amino groups have been made tertiary by substitution of the protons with picolyl moieties, as shown in Figure 1. A comparison between the reactivity of this complex and the iron(II) complex of the structurally related hexadentate ligand Fe(TPC)$^{2+}$ (TPC = 1,4,7-tripicolyl-1,4,7-triazacyclononane) with hydrogen peroxide and superoxide will be described in a subsequent paper.

Experimental Section

Materials. Solvents and reagents were the highest grade available and were found to be sufficiently pure for use as supplied. Where necessary, solvents were dried by prescribed techniques.[8]

Physical Techniques. UV–visible spectra were recorded on either a Varian 2300 spectrophotometer or a Hewlett Packard 8452 diode array spectrophotometer, with a 9000 (300) Hewlett Packard Chem Station. Both instruments incorporated flow through temperature-regulated cell holders connected to a Neslab constant-temperature circulation system, giving a temperature precision of ±0.3 °C.

All inert-atmosphere manipulations were performed in a dry nitrogen filled Vacuum Atmospheres Corp. (VAC) glovebox, equipped with a gas circulation and oxygen removal system, either a VAC MO40-1 or HE-493 dry train. Oxygen concentrations were maintained below 1 ppm.

(1) Chaudhuri, P.; Wieghardt, K. *Progress in Inorganic Chemistry*; Lippard, S. J, Ed.; Wiley: New York, 1987; Vol. 35; p 329.
(2) Hawker, P. N.; Twigg, M. V. *Comprehensive Coordination Chemistry*; Wilkinson, G., Gillard, R. D., McCleverty, J. A., Eds.; Pergamon Press: Oxford, U.K., 1987; Vol. 4.
(3) (a) Wieghardt, K.; Schmidt, W.; Herrman, W.; Küppers, H. J. *Inorg. Chem.* **1983**, *22*, 2953. (b) Boeyens, J. C. A.; Forbes, A. G. S.; Hancock, R. D.; Wieghardt, K. *Inorg. Chem.* **1985**, *24*, 2926.
(4) (a) Broan, C. J.; Jankowski, K. J.; Kataky, R.; Parker, D. *J. Chem. Soc., Chem. Commun.* **1990**, 1738. (b) Auerbach, U.; Eckert, U.; Wieghardt, K.; Nuber, B.; Weiss, J. *Inorg. Chem.* **1990**, *29*, 938. (c) Clarke, E. T.; Martell, A. E. *Inorg. Chim. Acta* **1991**, *186*, 103. (d) Wieghardt, K.; Bossek, U.; Chaudhuri, P.; Herrman, W.; Menke, B. C.; Weiss, J. *Inorg. Chem.* **1982**, *21*, 4308. (e) Hammershøi, A.; Sargeson, A. M. *Inorg. Chem.* **1983**, *22*, 3554. (f) Sayer, B. A.; Michael, J. P.; Hancock, R. D. *Inorg. Chim. Acta* **1983**, *77*, L63. (g) Alcock, N. W.; McLaren, F.; Moore, P.; Pike, G. A.; Roe, S. M. *J. Chem. Soc., Chem. Commun.* **1989**, 629. (h) Ziessel, R.; Lehn, J.-M. *Helv. Chim. Acta* **1990**, *73*, 1449. Peacock, R. D.; Robb, *J. Inorg. Chim. Acta* **1986**, *121*, L15. Belal, A. A.; Farrugia, L. J.; Peacock, R. D.; Robb, J. *J. Chem. Soc., Dalton Trans.* **1989**, 931.
(5) (a) Beissel, T.; Della Vedova, B. S. P. C.; Wieghardt, K.; Boese, R. *Inorg. Chem.* **1990**, *29*, 1736. (b) Wieghardt, K.; Chaudhuri, P.; Nuber, B.; Weiss, J. *Inorg. Chem.* **1982**, *21*, 3086.
(6) (a) Boeyens, J. C. A.; Hancock, R. D.; Thôm, V. J. *J. Crystallogr. Spectrosc. Res.* **1984**, *14*, 261. (b) Hancock, R. D.; Thôm, V. J. *J. Am. Chem. Soc.* **1982**, *104*, 291. (c) Flassbeck, C.; Wieghardt, K.; Bill, E.; Butzlaff, C.; Trautwein, A. X.; Nuber, B.; Weiss, J. *Inorg. Chem.* **1992**, *31*, 21.
(7) (a) Boeyens, J. C. A.; Dobson, S. M.; Hancock, R. D. *Inorg. Chem.* **1985**, *24*, 3073. (b) Hancock, R. D.; Dobson, S. M.; Boeyens, J. C. A. *Inorg. Chim. Acta* **1987**, *133*, 221.
(8) Mann, C. K. *Electroanal. Chem.* **1969**, *3*, 58.

0020-1669/93/1332-0297$04.00/0

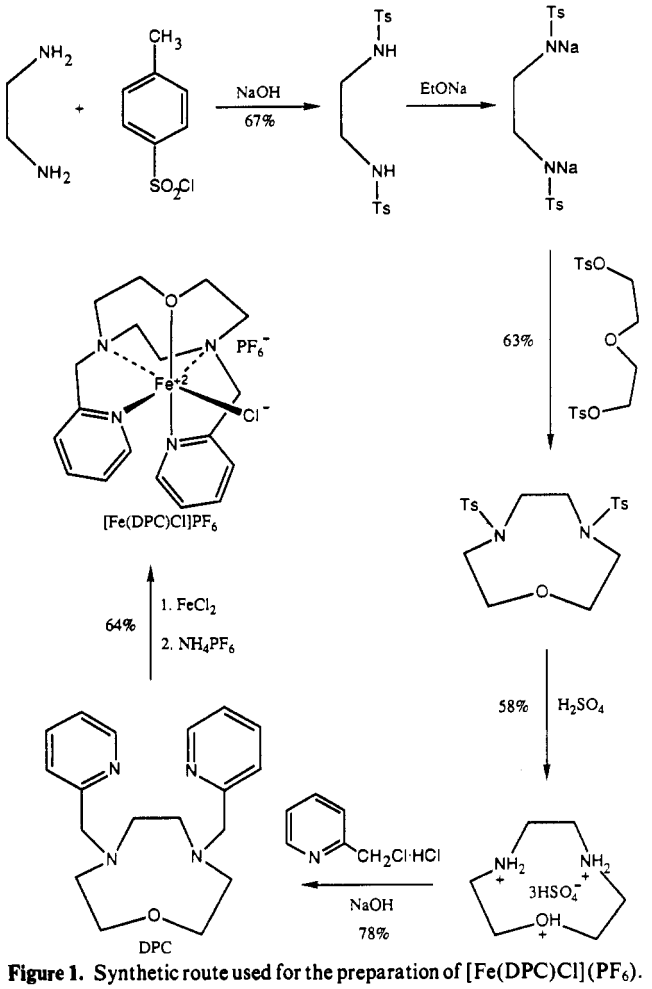

Figure 1. Synthetic route used for the preparation of [Fe(DPC)Cl](PF_6).

Proton and ^{13}C NMR spectra were obtained with a GE QE 300 plus spectrometer. All NMR spectra were obtained in deuterated solvent solution. ESR spectra were recorded with a Varian E-112 spectrometer operating in the X-band. Samples were run as a frozen glass in a round quartz tube submerged in liquid nitrogen (77 K). Infrared spectra were acquired using a Perkin-Elmer 1600 FTIR spectrometer with Perkin-Elmer ATR equipment on either a KRS-5 or a germanium crystal as the reflection element. Mass spectra (fast atom bombardment) were obtained using a VG ZAB HS mass spectrometer equipped with a xenon gun. Several matrices were used, including NAB (nitrobenyl alcohol) and TG/G (thioglycerol/glycerol).

Electrochemical experiments were performed using a three-compartment cell. The working electrode was either a 3-mm-diameter glass-carbon electrode in Kel-F (Bioanalytical systems) or a polished glassy-carbon plate (Tokai Carbon Co., Ltd.) of surface area = 1.05 cm^2; the secondary electrode was a platinum wire separated by a glass frit from the working electrode compartment, and the reference electrode was Ag/AgCl, in the solvent of the experiment with supporting electrolyte, separated from the main compartment by a capillary formed by sealing a platinum wire in glass. The potential of the reference electrode was determined by the cyclic voltammetry of known reversible redox couple, $E_{Ag/AgCl}$ = 0.19 V vs NHE in 4 M KCl. The experiments were undertaken using a Princeton Applied Research (PAR) programmer Model 175 and PAR potentiostat Model 173, and the output was directly recorded on paper using a Houston Instruments Model 200 XY recorder. Aqueous solutions typically contained 0.1 M KCl as supporting electrolyte, and in nonaqueous solvents, the supporting electrolyte was 0.1 M tetrabutylammonium tetrafluoroborate (TBAB) (Southwestern Analytical Chemicals, Electrometric grade).

Spectroelectrochemical experiments (SEC) were performed by using closely spaced polished glassy-carbon (Tokai Carbon Co. Ltd.) electrodes parallel to the optical beam. The design of the cell, shown in Figure 2,, is a modification of a previously designed long path thin-layer spectroelectrochemical cell.[9] Futher details of spectroelectrochemical techniques may be found elsewhere.[10]

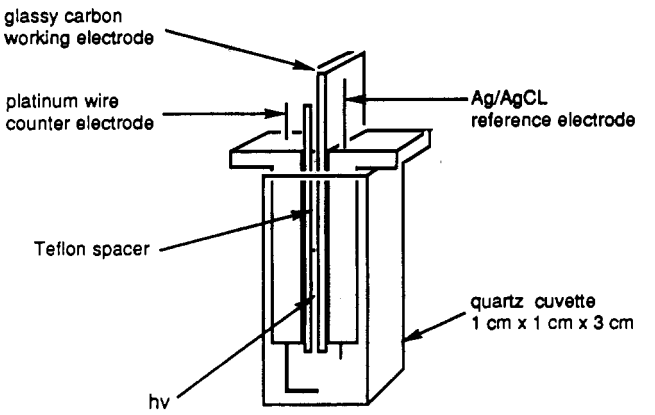

Figure 2. Diagram showing long path length, thin-layer spectroelectrochemical cell.

X-ray Structure Determination. Crystals of [Fe(DPC)Cl]PF_6 were obtained from methanol. Character: golden-yellow plates. A thin lath was chosen for data collection. Data were collected with a Siemens R3m four-circle diffractometer in the ω-2θ mode. The maximum 2θ was 50° with scan range ±0.7° (ω) around the $K_{\alpha1}$–$K_{\alpha2}$ angles, with scan speed 2–15° (ω) min^{-1}, depending on the intensity of a 2-s prescan; backgrounds were measured at each end of the scan for 0.25 of the scan time. *hkl* ranges were 0/9, 0/15, and 0/24.

Three standard reflections were monitored every 200 reflections and showed no significant decrease during data collection. Unit cell dimensions and standard deviations were obtained by least-squares fit to 15 reflections ($18 < 2\theta < 20°$). The 2234 reflections collected (all unique) were processed using profile analysis: 1895 were considered observed ($I/\sigma(I) \geq 2.0$). These were corrected for Lorentz, polarization, and absorption effects (by the Gaussian method); minimum and maximum transmission factors were 0.85 and 0.91. Crystal dimensions were 0.21 × 0.11 × 0.97 mm.

Systematic reflection conditions *h*00, $h = 2n$; 0*k*0, $k = 2n$; and 00*l*, $l = 2n$, indicate space group $P2_12_12_1$. The structure was solved by direct methods using SHELXTL (TREF).[11] Anisotropic thermal parameters were used for all non-H atoms. Hydrogen atoms were given fixed isotropic thermal parameters, U = 0.08 Å^2, which were inserted at calculated positions and not refined. The absolute structure of the individual crystal chosen was checked by refinement of a $\delta f''$ multiplier. Final refinement was on F by least-squares methods refining 289 parameters. The largest positive and negative peaks on a final difference Fourier synthesis was of height ±0.5 e Å^{-3}.

A weighting scheme of the form $W = 1/(\sigma^2(F) + gF^2)$ with $g = 0.0024$ was used and shown to be satisfactory by a weight analysis. Final R = 0.049, R_w = 0.069, and S = 1.18; R(all reflections) = 0.059. The maximum shift/error in the final cycle was 0.03. Computing was done with SHELXTL PLUS[12] on a DEC Microvax-II. Scattering factors in the analytical form and anomalous dispersion factors were taken from ref 13. Final atomic coordinates are given in Table I, and selected bond lengths and angles in Tables II and III.[14]

Synthesis of 4,7-Bis(2-picolyl)-4,7-diaza-1-oxacyclononane, DPC. The parent macrocycle, [9]aneON$_2$, was prepared by the method of Hancock and Thöm, as outlined in Figure 1,[6b] and DPC was prepared by addition of an aqueous solution (10 mL) of 2-picolyl chloride hydrochloride (1.5 g, 9 mM) dropwise to an aqueous solution (20 mL) of [9]aneON$_2$·3H$_2$SO$_4$ (0.6 g, 4.5 mM), which had been neutralized to pH = 7 with 0.5 N NaOH, with stirring over a period of 1 h at room temperature. The pH of the solution was adjusted to 9.0 with 0.5 M NaOH, after which the

(9) (a) Pruiksma, R.; McCreery, R. L. *Anal. Chem.* **1981**, *53*, 202. (b) Gui, Y.-P.; Porter, M. D.; Kuwana, T. *T. Anal. Chem.* **1985**, *57*, 1474. (c) Gui, Y.-P.; Kuwana, T. *Anal. Chem.* **1986**, *2*, 471. (d) Tyson, J. F. *Talanta* **1986**, *33*, 51.
(10) Heineman, W. R.; Hawkridge, F. M.; Blount, H. N. *Electroanalytical Chemistry*; Bard, A. J., Ed.; Marcel Dekker: New York, 1984; Vol. 13, pp 1–109.
(11) Sheldrick, G. M. *SHELXTL user's manual*; Nicolet Instr. Co.: Madison, WI, 1983.
(12) Sheldrick, G. M. *SHELXTL Plus user's manual*; Nicolet Instr. *Co.*: Madison, WI, 1986.
(13) *International Tables for X-Ray Crystallography*; Kynoch Press: Birmingham, U.K., 1974; Vol. IV (present distributor Kluwer Academic Publishers, Dordrecht, The Netherlands).
(14) (a) Evans, D. F. *J. Chem. Soc.* **1959**, 2003. (b) Sur, S. K. *J. Magn. Reson.* **1989**, *82*, 169.

Table I. Atom Coordinates ($\times 10^4$) and Isotropic Thermal Parameters ($Å^2 \times 10^3$)

atom	x	y	z	U^a
Fe(1)	1442.6 (12)	6535.8 (7)	2169.0 (4)	28 (1)
Cl(1)	3809.6 (23)	7506.8 (15)	2021.3 (9)	47 (1)
O(1)	928 (6)	7309 (3)	3129 (2)	36 (2)
C(2)	−768 (9)	7283 (6)	3363 (4)	42 (2)
C(3)	−1875 (9)	6982 (5)	2783 (3)	37 (2)
N(4)	−1206 (8)	6097 (4)	2433 (3)	35 (2)
C(5)	−1243 (10)	5162 (5)	2814 (4)	36 (2)
C(6)	423 (9)	4616 (5)	2795 (4)	37 (2)
N(7)	1843 (7)	5329 (4)	2896 (3)	34 (2)
C(8)	1915 (10)	5705 (6)	3570 (3)	40 (2)
C(9)	2104 (11)	6856 (6)	3577 (4)	45 (2)
C(11)	−2055 (10)	5978 (6)	1805 (4)	41 (2)
C(12)	−1575 (9)	6814 (5)	1347 (3)	36 (2)
N(13)	21 (7)	7123 (4)	1366 (3)	33 (2)
C(14)	505 (11)	7837 (5)	958 (3)	40 (2)
C(15)	−555 (12)	8272 (7)	494 (4)	52 (3)
C(16)	−2168 (13)	7994 (7)	500 (5)	59 (3)
C(17)	−2686 (11)	7243 (7)	912 (4)	51 (3)
C(21)	3438 (10)	4857 (6)	2702 (4)	41 (2)
C(22)	3490 (9)	4694 (5)	1973 (3)	32 (2)
N(23)	2451 (8)	5270 (4)	1612 (3)	32 (2)
C(24)	2465 (11)	5139 (6)	968 (4)	41 (2)
C(25)	3488 (11)	4471 (6)	658 (4)	44 (2)
C(26)	4569 (12)	3910 (7)	1016 (5)	55 (3)
C(27)	4609 (11)	4009 (6)	1681 (4)	42 (3)
P(1)	6365.3 (32)	5655.1 (21)	4741.6 (11)	58 (1)
F(1)	6068 (9)	5984 (8)	4027 (3)	133 (4)
F(2)	7309 (20)	6658 (9)	4841 (6)	189 (6)
F(3)	6602 (12)	5420 (12)	5457 (4)	188 (6)
F(4)	5311 (20)	4769 (9)	4688 (6)	214 (8)
F(5)	4668 (14)	6192 (13)	4875 (5)	207 (8)
F(6)	8038 (12)	5226 (11)	4565 (6)	186 (6)

[a] Equivalent isotropic U defined as one-third of the trace of the orthogonalized U_{ij} tensor.

Table II. Bond Lengths (Å)

Fe(1)–Cl(1)	2.309 (3)	Fe(1)–O(1)	2.257 (5)
Fe(1)–N(4)	2.266 (7)	Fe(1)–N(7)	2.206 (6)
Fe(1)–N(13)	2.149 (6)	Fe(1)–N(23)	2.179 (6)
O(1)–C(2)	1.442 (9)	O(1)–C(9)	1.447 (9)
C(2)–C(3)	1.537 (10)	C(3)–N(4)	1.473 (9)
N(4)–C(5)	1.461 (9)	N(4)–C(11)	1.466 (10)
C(5)–C(6)	1.518 (10)	C(6)–N(7)	1.491 (9)
N(7)–C(8)	1.471 (9)	N(7)–C(21)	1.477 (10)
C(8)–C(9)	1.525 (11)	C(11)–C(12)	1.500 (10)
C(12)–N(13)	1.343 (9)	C(12)–C(17)	1.383 (11)
N(13)–C(14)	1.320 (9)	C(14)–C(15)	1.399 (12)
C(15)–C(16)	1.344 (14)	C(16)–C(17)	1.367 (13)
C(21)–C(22)	1.513 (10)	C(22)–N(23)	1.349 (9)
C(22)–C(27)	1.408 (11)	N(23)–C(24)	1.333 (10)
C(24)–C(25)	1.362 (11)	C(25)–C(26)	1.357 (12)
C(26)–C(27)	1.372 (12)	P(1)–F(1)	1.548 (7)
P(1)–F(2)	1.537 (13)	P(1)–F(3)	1.515 (9)
P(1)–F(4)	1.447 (14)	P(1)–F(5)	1.558 (13)
P(1)–F(6)	1.500 (11)		

resulting orange solution was extracted (3 × 50 mL) with $CHCl_3$. After being washed with water, the collected organic layers, which contained the product, were dried over Na_2SO_4, and the solvent was removed under reduced pressure. The product was a brown oil. Yield: 1.1 g (78%). A mass spectrum displayed the expected molecular ion peak for $[C_{18}H_{24}N_4O]^+$ at $m/z = 312$. An IR spectrum of the compound showed strong bands at 2920 and 1569 cm^{-1}, as found in TPC. Moreover, the spectrum displayed strong bands at 1124 and 1046 cm^{-1} assignable to the ether group and at 750 cm^{-1} due to the ortho-substituted pyridine rings. The ^1H NMR spectrum (in CD_3CN) exhibited peaks at $\delta = 2.90$ (s, 4H); 2.96 (t, 3H), 3.72 (t, 4H), and 3.89 ppm (s, 4H) and two triplets and two doublets between $\delta = 7.10$ and 8.60 ppm from the eight protons of the two pyridine rings. The ^{13}C NMR spectrum (in CD_3CN) showed nine peaks at $\delta = 55.30$, 55.32, 64.12, 72.49, 121.82, 123.08, 136.26, 148.94, and 160.21 ppm.

Preparation of Chloro(4,7-bis(2-picolyl)-4,7-diaza-1-oxacyclononane)-iron(II) Hexafluorophosphate, [Fe(DPC)Cl]PF_6. Under N_2, DPC (0.55 g, 1.76 mM) and $FeCl_2 \cdot 4H_2O$ (0.35 g, 1.76 mM) were dissolved in 50 mL of MeOH, resulting in a brown solution, which was heated to 60 °C and stirred for 3 h. NH_4PF_6 (0.54 g, 3.52 mM, in 30 mL of MeOH) was added to the solution. The reaction mixture was placed in a refrigerator at −10 °C for 24 h in order to crystallize the product. The resulting yellow crystals were dissolved in acetone, and the solution was filtered. The product was precipitated again by adding diethyl ether and recrystallized from methanol. Yield: 0.62 g (64%). Anal. Calcd for $C_{18}H_{24}N_4OFeClPF_6$: C, 39.40; H, 4.41; N, 10.21. Found: C, 39.16; H, 4.80; N, 10.03. The mass spectrum (FAB in NBA) displayed a molecular ion peak for $[C_{18}H_{24}N_4OFeCl]^+$ at $m/e = 403$. The electronic spectrum of a dilute solution in MeCN exhibited two absorption bands with maxima at $\lambda_{max} = 260$ and 398 nm ($\epsilon = 9.6 \times 10^3$ and 2.4×10^3 M^{-1} cm^{-1}, respectively). The IR spectrum (ATR with KRS-5) of the complex showed a band at 1608 cm^{-1}, characteristic of the skeletal vibration of the pyridine rings, and strong bands at 840 and 558 cm^{-1}, arising from PF_6^-.

Table III. Bond Angles (deg)

Cl(1)–Fe(1)–O(1)	90.8 (1)	Cl(1)–Fe(1)–N(4)	160.5 (2)
O(1)–Fe(1)–N(4)	74.6 (2)	Cl(1)–Fe(1)–N(7)	111.7 (2)
O(1)–Fe(1)–N(7)	76.2 (2)	N(4)–Fe(1)–N(7)	77.9 (2)
Cl(1)–Fe(1)–N(13)	97.8 (2)	O(1)–Fe(1)–N(13)	114.2 (2)
N(4)–Fe(1)–N(13)	77.2 (2)	N(7)–Fe(1)–N(13)	148.9 (2)
Cl(1)–Fe(1)–N(23)	92.9 (2)	O(1)–Fe(1)–N(23)	150.7 (2)
N(4)–Fe(1)–N(23)	106.1 (2)	N(7)–Fe(1)–N(23)	75.4 (2)
N(13)–Fe(1)–N(23)	94.0 (2)	Fe(1)–O(1)–C(2)	116.9 (4)
Fe(1)–O(1)–C(9)	104.5 (4)	C(2)–O(1)–C(9)	113.1 (5)
O(1)–C(2)–C(3)	107.0 (6)	C(2)–C(3)–N(4)	111.9 (6)
Fe(1)–N(4)–C(3)	104.8 (4)	Fe(1)–N(4)–C(5)	111.3 (5)
C(3)–N(4)–C(5)	113.5 (5)	Fe(1)–N(4)–C(11)	104.6 (4)
C(3)–N(4)–C(11)	110.2 (6)	C(5)–N(4)–C(11)	111.8 (6)
N(4)–C(5)–C(6)	111.6 (6)	C(5)–C(6)–N(7)	111.6 (6)
Fe(1)–N(7)–C(6)	104.5 (4)	Fe(1)–N(7)–C(8)	113.5 (4)
C(6)–N(7)–C(8)	111.9 (6)	Fe(1)–N(7)–C(21)	104.3 (4)
C(6)–N(7)–C(21)	110.9(5)	C(8)–N(7)–C(21)	111.2 (6)
N(7)–C(8)–C(9)	110.4 (6)	O(1)–C(9)–C(8)	109.9 (6)
N(4)–C(11)–C(12)	110.8 (6)	C(11)–C(12)–N(13)	116.6 (6)
C(11)–C(12)–C(17)	122.8 (7)	N(13)–C(12)–C(17)	120.6 (7)
Fe(1)–N(13)–C(12)	114.8 (5)	Fe(1)–N(13)–C(14)	126.1 (5)
C(12)–N(13)–C(14)	118.5 (6)	N(13)–C(14)–C(15)	123.1 (8)
C(14)–C(15)–C(16)	117.8 (8)	C(15)–C(16)–C(17)	119.7 (9)
C(12)–C(17)–C(16)	120.0 (8)	N(7)–C(21)–C(22)	110.5 (6)
C(21)–C(22)–N(23)	116.6 (6)	C(21)–C(22)–C(27)	122.0 (6)
N(23)–C(22)–C(27)	121.4 (6)	Fe(1)–N(23)–C(22)	111.8 (4)
Fe(1)–N(23)–C(24)	128.6 (5)	C(22)–N(23)–C(24)	117.8 (6)
N(23)–C(24)–C(25)	123.7 (7)	C(24)–C(25)–C(26)	118.9 (8)
C(25)–C(26)–C(27)	120.2 (8)	C(22)–C(27)–C(26)	118.1 (7)
F(1)–P(1)–F(2)	87.8 (6)	F(1)–P(1)–F(3)	175.2 (7)
F(2)–P(1)–F(3)	89.2 (7)	F(1)–P(1)–F(4)	93.7 (6)
F(2)–P(1)–F(4)	173.1 (8)	F(3)–P(1)–F(4)	88.9 (7)
F(1)–P(1)–F(5)	84.5 (5)	F(2)–P(1)–F(5)	90.9 (8)
F(3)–P(1)–F(5)	91.8 (6)	F(4)–P(1)–F(5)	82.5 (8)
F(1)–P(1)–F(6)	90.8 (5)	F(2)–P(1)–F(6)	85.2 (8)
F(3)–P(1)–F(6)	92.6 (6)	F(4)–P(1)–F(6)	101.5 (8)
F(5)–P(1)–F(6)	174.0 (7)		

Results and Discussion

The ligand DPC is prepared in high yield by reaction of [9]-aneON$_2$ with 2-picolyl chloride hydrochloride in aqueous solution. The iron(II) complex was readily prepared by mixing equimolar amounts of iron(II) chloride with the free ligand in methanol, anaerobically. The mixed chloride–hexafluorophosphate salt was isolated by filtration of the precipitate that formed upon addition of $[NH_4][PF_6]$, as shown in Figure 1.

X-ray Crystal Structure. The crystallographic data confirm a pseudo-octahedral structure for [Fe(DPC)Cl]PF_6, with the chloride ligated *trans* to a nitrogen atom of the pentadentate ligand. Figure 3 shows two perspective views of the structure. In Figure 3a the viewer looks down the Cl–Fe–N axis, and in Figure 3b the viewer looks down what would be the 3-fold axis in a more ideal structure. The latter shows that the py$_2$Cl set of ligands are rotated from the ideal 60° of an octahedron to an average of 31°, midway between an octahedral and a trigonal prismatic structure. Comparison with data for tris(2-pyridyl)-triazacyclononane (TPC) is revealing. For low-spin $[Fe(TPC)]^{2+}$, $[Ni(TPC)]^{2+}$, and $[Mn(TPC)]^{2+}$, the corresponding angle de-

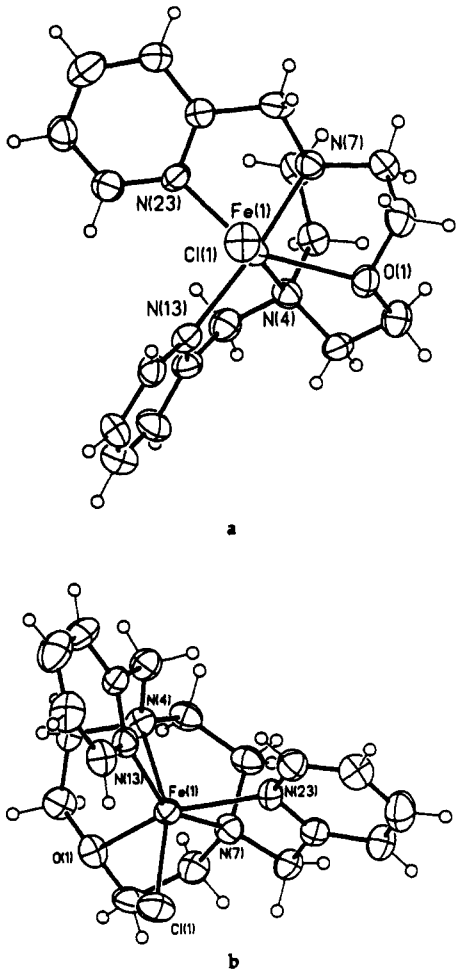

Figure 3. Ortep diagram of $[Fe(DPC)Cl]PF_6$.

creases as the size of the metal ion increases; the shift toward the trigonal prismatic structure is driven by the need to minimize the strain energy of the ligand. Therefore it is not surprising that the relatively large, high-spin iron(II) in $[Fe(DPC)Cl]^{2+}$ produces a small dihedral angle on this hypothetical 3-fold axis (average Fe–N distance, 2.20 Å). The DPC ligand also produces a distortion of the hypothetical 4-fold axes of the pseudo-octahedron about iron; the N(7)–Fe–N(13), N(23)–Fe–O, and N(4)–Fe–Cl angles are 148.9, 150.7, and 160.5°, respectively, the donor atoms of the first two being drawn back toward the cyclononane part of the structure. It is interesting that the Fe–O distance, 2.257 (5) Å, is similar to the longest Fe–N distance, 2.266 (7) Å. The bond distances and angles (Tables II and III) are otherwise unremarkable.

Magnetic Properties. An ^1H NMR spectrum (in CD_3CN) of $Fe(DPC)^{2+}$ showed peaks only for the solvent and water indicating paramagnetic broadening due to the presence of unpaired electrons. Two ESR spectra (in CH_3CN) of $Fe(DPC)^{2+}$ were recorded, one at 77 and the other at 298 K. In neither spectrum was a resonance observed, indicating that if the iron(II) complex is high spin, the relaxation time is very short. These data were supported by a susceptibility measurement using ^1H NMR (Evans method).[14] The magnetic moment of $Fe(DPC)^{2+}$ at 25 °C was found to be 4.92 μ_B, indicating four unpaired electrons and a spin S of 2. This value suggests that the complex may be 6-coordinated in solution, probably with a coordinated anion or solvent molecule. The high-spin state of this complex is consistent with its yellow color in both the solid and solution states.[15] The iron(II) complexes

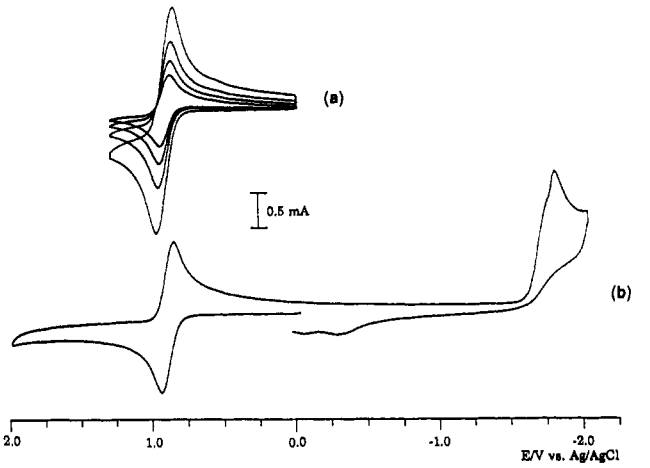

Figure 4. Cyclic voltammogram of 1.8 mM $[Fe(DPC)Cl](PF_6)$ in acetonitrile containing 0.1 M Bu_4NBF_4 at a glass-carbon electrode: (a) at sweep rates of 20, 50, 100, and 200 mV/s; (b) at a sweep rate of 100 mV/s.

of substituted triazacyclononane and related ligands are apparently close to the spin crossover point. For example (1,4,7-tripicolyl-1,4,7-triazacyclononane)iron(II) has been reported to be low spin, with a μ value of 1.20–1.26 μ_B (303–406 K)[15] and 0.26–0.63 μ_B (298 K).[16] In contrast (1,4,7-triacetato-1,4,7-triazacyclononane)iron(II) is high-spin μ = 5.6 μ_B.[4b] The crystallographic data for the high-spin $Fe(DPC)^{2+}$ reveals an octahedral structure rather than the square pyramidal structure of the analogous copper(II) complex of the thio analogue (4,7-bis(pyridylmethyl)-1-thia-4,7-diazacyclononane.[17]

Electrochemical Properties. In acetonitrile solution containing 0.1 M TBAB, the iron(III/II) redox couple for $[Fe(DPC)Cl]PF_6$ is reversible and appears at $E_{1/2}$ = 0.71 V vs NHE (0.52 V vs Ag/AgCl); the i_{pa}/i_{pc} ratio was found to be 1, and ΔE_p = 60 mV. The number of electrons (n) involved in the redox process was determined using the Malachesky equation,[18] which relates the number of electrons to the square of the ratio of the slopes from a Randles plot of the peak current versus the square root of the cyclic voltammetry sweep rate, and a Cottrell's plot of current versus inverse square root of time from a potential step chronoamperometric experiment.[19] It was found that n = 0.96 ± 0.05, and the diffusion coefficient $D = 7.6 \times 10^{-6}$ cm^2 s^{-1}, respectively. Further, a two-step irreversible reduction process was also observed (Figure 4) and assigned to reduction of the ligand, E_{cp} = −1.75 and −1.9 V vs Ag/AgCl, by comparison to the cyclic voltammetry of the free ligand (in DMF) (reductive process, E_{pc} = −1.130 and −1.65 V, and oxidative processes, E_{pa} = 0.82 and 1.18 V vs Ag/AgCl). The ligand oxidation processes were absent from the cyclic voltammogram of the metal complex performed over the same potential range; presumably the ligand is stabilized against oxidation by coordination to the metal center.

On the basis of the reversibility of the iron(II/III) redox couple, it is apparent that the iron(III) form of this complex is stable in acetonitrile solution, at least on the time scale of the cyclic voltammetric measurements. An ESR spectrum at 77 K of $Fe(DPC)^{3+}$, produced by electrooxidation in acetonitrile, exhibits two signals; the first at g_1 = 9.324, g_2 = 8.291, and g_3 = 5.776, Figure 5, is consistent with a high-spin iron(III) species with rhombic distortion, and the second at g = 4.532 has been associated

(15) Christiansen, L.; Hendrickson, D. N.; Toftlund, H.; Wilson, S. R.; Xie, C. L. *Inorg. Chem.* **1986**, *25*, 2813.
(16) Wieghardt, K.; Schöffmann, E.; Nuber, B.; Weiss, B. J. *Inorg. Chem.* **1986**, *25*, 4877.
(17) Wasielewski, K.; Mattes, R. *Acta Crystallogr.* **1990**, *C46*, 1826.
(18) Malachesky, P. A. *Anal. Chem.* **1969**, *41*, 1493.
(19) Bard, A. J.; Faulkner, L. R. *Electrochemical Methods*; Wiley: New York, 1980.

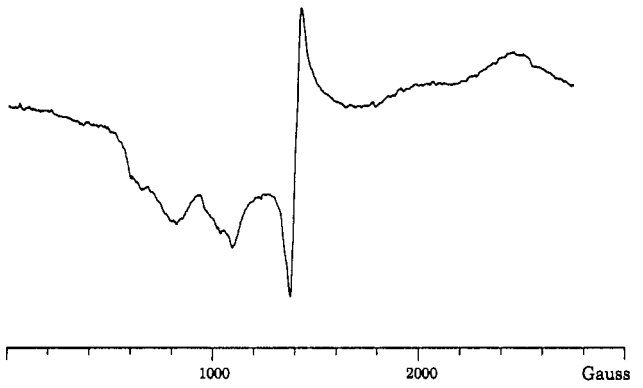

Figure 5. ESR spectrum of $[Fe^{III}(DPC)Cl](PF_6)^+$ in acetonitrile, measured at 77 K.

with structures deviating strongly from cubic symmetry.[20] Again, the sixth coordination site may be occupied by either chloride or solvent.

Cyclic voltammograms of $[Fe(DPC)Cl]PF_6$, dissolved in 2 M aqueous KCl, for scan rates $v > 0.2$ V/s exhibit a quasi-reversible redox process at $E_{1/2} = 0.81$ V vs NHE with $\Delta E_p = 80$ mV that is assigned to the Fe(II/III) redox couple. However, for scan rates slower than 200 mV/s the i_{pa}/i_{pc} ratio was approximately 2:3 and an additional redox couple was observed at $E_{1/2} = 0.54$ V vs NHE, indicating that the complex is unstable in aqueous solution, perhaps undergoing hydrolysis to a hydroxo complex.

At high chloride concentrations in aqueous solution (2 M KCl), the cyclic voltammograms of $Fe(DPC)^{2+}$ exhibit an almost reversible iron(III/II) redox couple indicating that the iron(III) complex formed upon oxidation is structurally very similar to the initial iron(II) complex, $[Fe(III)(DPC)L]^{2+}$, where L is either H_2O or Cl^-. In order to examine this process is more detail, cyclic voltammograms of $Fe(DPC)^{2+}$ in 2 M aqueous KCl were measured over a range of pH values. Below pH = 7, the iron(III/II) redox couple is quasi-reversible; however, at higher pH, two reduction processes may be observed in the cathodic sweep, indicating the presence of at least two iron(III) species. For pH values greater than 9.4, the iron(III/II) redox couple is again quasi-reversible but with the redox potential at a more negative potential than occurred for neutral solution, as shown in Figure 6. These results indicate the presence of an equilibrium between various forms of the iron(III) complex, probably arising from competition between chloride and hydroxide for the sixth iron(III) coordination site.

In order to examine the above proposal, a potentiometric experiment was undertaken, measuring the potential over a range of pH values. The graph of potential measured versus pH was linear, with a slope of 52 mV per pH unit. Assuming an equilibrium reaction of the form

$$Fe^{III}L + nH_2O \rightleftharpoons Fe^{III}L(OH)_n + nH^+$$

and combining this with the Nernst equation describing the iron(III/II) redox couple, it may be shown that a graph of observed iron(III/II) redox potential versus pH would have a slope of 59 mV for $n = 1$ in RT. The potentiometric result indicates that there is a net one proton change per electron (iron) in the oxidation process. The quasi-reversibility of the cyclic voltammograms of the $Fe(DPC)^{2+}$ complex at high pH indicate that iron(III) exists as hydroxy complex rather than a μ-oxo dimer, since it is unlikely

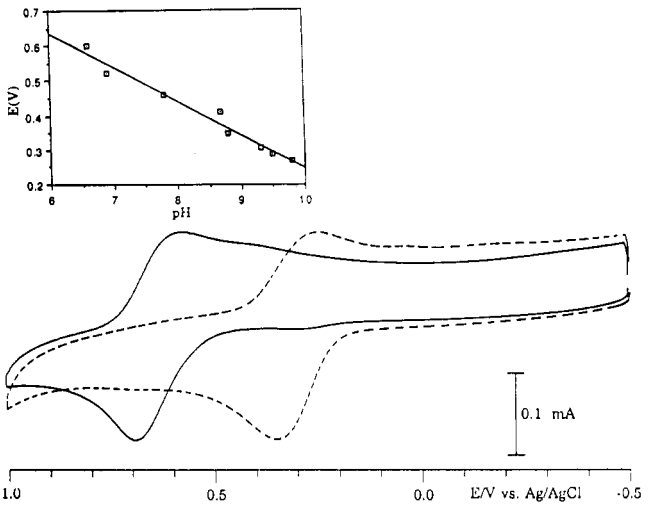

Figure 6. Cyclic voltammograms of 0.1 mM $[Fe(DPC)Cl](PF_6)$ in aqueous 2 M KCl, with a sweep rate of 100 mV/s at a glassy-carbon electrode, at pH = 5.6 and pH = 9.6.

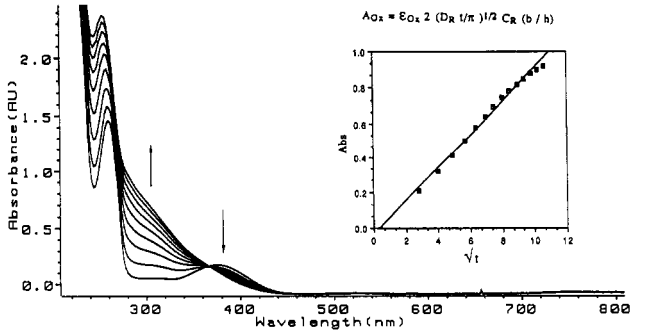

Figure 7. UV–visible spectral changes occurring during spectroelectrochemical study of the oxidation of 0.075 mM $[Fe(DPC)Cl](PF_6)$ in aqueous 2 M KCl, at a glassy-carbon electrode, following a potential step from 0.0 to 0.7 V vs Ag/AgCl. The insert shows a plot of absorbance at 312/nm versus the square root of time following potential step (b = length of electrode surface traversed by beam; h = thickness of the beam; and other symbols have their usual meanings).[9d]

that the μ-oxo dimer would remain intact for the iron(II) oxidation state. Possibly, μ-oxo dimer formation is prevented by the steric hindrance about the iron.

A spectroelectrochemical examination of the Fe(III/II) redox couple revealed that, upon oxidation of $[Fe(DPC)Cl]^+$ in 2 M aqueous KCl, the metal ligand charge-transfer band at λ_{max} = 378 nm disappeared, whereas the band at 260 nm assigned as a ligand π to π^* transition shifted to higher energy at λ_{max} = 254 nm. Furthermore, during the oxidation process, there was a concomitant increase in absorbance with λ_{max} = 312 nm, as shown in Figure 7. As discussed above, the cyclic voltammetry indicates that oxidation of $[Fe^{II}(DPC)Cl]^+$ under conditions of high chloride concentration produces almost exclusively $[Fe^{III}(DPC)Cl]^{2+}$. This conclusion is further supported by the spectroelectrochemical results. The spectral changes occurring upon oxidation may be fully reversed on applying a potential negative of the iron(III/II) redox couple, and the sharp isosbestic point λ = 364 nm indicates that the oxidation process involves only two major species. From these results the UV–visible spectrum of $[Fe^{III}(DPC)Cl]^{2+}$ in aqueous chloride is apparent (λ_{max} = 256 and 312 nm, ϵ = 35.0 and 11.1×10^3 M^{-1} cm^{-1}, respectively). The number of electrons for the oxidation process may be calculated by measuring the spectra at steady state over a potential range near the iron(III/II) redox potential (spectropotentiostatic) and fitting the absorbance changes to the Beer–Lambert/Nernst equations. The value of n obtained by this method ($n = 1.0 \pm 0.05$) is in good agreement with that obtained from cyclic voltammetry as discussed above.

(20) (a) Bencini, A.; Gatteschi, D. *Transition Metal Chemistry*; Melson, G. A., Figgis, B. N., Eds.; Marcel Dekker: New York and Basel, 1983; Vol. 8, p 87. (b) Palmer, G. *Iron Porphyrins, Part II*; Lever, A. B. P., Gray, H. B., Eds.; Addison-Wesley Publ. Co.: London, 1983; pp 43–88. (c) Blumberg, W. E. *Magnetic Resonance in Biological Systems*; Ehrenberg, A., Malmstrom, B. G., Vanngard, T., Eds.; Pergamon Press: New York, 1967; pp 119–33.

The redox potential of $Fe(DPC)^{2+}$ is relatively positive compared to many iron(II) complexes of substituted triazacyclononane and related species, such as bis(triazacyclononane)-iron(II) (E = 0.13 V vs NHE in 0.1 M aqueous KCl, 23 °C),[3a] resulting in the observed stability of $Fe^{II}(DPC)^{2+}$ in the presence of oxygen. The effect of having ligating substituents on the triazacyclonone typically results in complexes containing only one ligand per iron. The iron(III/II) redox potential is very dependent upon the nature of the substituent, a result common to many families of iron(II) macrocyclic complexes.[21] For example for the hexadentate 1,4,7-tri-X-substituted cyclononanes, the iron(III/II) redox potential E = −1.45 V vs NHE in CH_2Cl_2 for X = 3-*tert*-butyl-2-hydroxybenzyl,[22] E = +0.195 V vs NHE for X = acetate,[4d] and E = 0.76 V vs NHE in acetonitrile for X = 2-pyridylmethyl.[16] Substitution of a triazacyclononane nitrogen by an oxygen may be expected to lower the affinity of the macrocycle for iron(II) as observed by Hancock and Thöm[6b] for the stability constants of [9]aneN_3 and [9]aneN_2O with nickel(II) (log K_{ML} = 16.24[6b] and 8.59[23]), respectively. The effect of redox potential is determined by the relative influences of ligand substitution on the stabilities of the iron(II) and iron(III) complexes. It may be expected that the presence of oxygen would favor the iron(II) oxidation state. Presumably this effect almost equals the potential change expected on exchanging a chelated pyridyl group for a ligated chloride, since the iron(III/II) potentials of DPC and 1,4,7-tris(2-pyridylmethyl)triazacyclononane[16] are very similar (0.71 and 0.74 V vs NHE in acetonitrile, respectively). This result is extremely fortuitous, since it allows any difference in the reactivity of these two iron(II) complexes to be ascribed to other structural features of the complexes; the subject of a subsequent paper.

Acknowledgment. The financial support of Monsanto is greatly appreciated.

Supplementary Material Available: Lists of anisotropic thermal parameters and H-atom coordinates (2 pages). Ordering information is given on any current masthead page.

(21) Busch, D. H.; Pillsbury, D. G.; Lovecchio, F. V.; Tait, A. M.; Hung, Y.; Jackels, S.; Rakowski, M. C.; Schammel, W. P.; Martin, L. Y. *Electrochemical Studies of Biological Systems*; Sawyer, D. T., Ed.; ACS Symposium Series No. 38; American Chemical Society: Washington, DC, 1977.

(22) Auerbach, U.; Eckert, U.; Wieghardt, K.; Nuber, B.; Weiss, J. *Inorg. Chem.* **1990**, *29*, 938.

(23) Yang, R.; Zompa, L. J. *Inorg. Chem.* **1976**, *15*, 1499.